FUNCTIONAL ORGANIZATION OF MITOTIC MICROTUBULES

PHYSICAL CHEMISTRY OF THE IN VIVO EQUILIBRIUM SYSTEM

SHINYA INOUÉ, JOHN FUSELER, EDWARD D. SALMON, *and* GORDON W. ELLIS

From the Program in Biophysical Cytology, Department of Biology, University of Pennsylvania, Philadelphia, Pennsylvania 19174, and Marine Biological Laboratories, Woods Hole, Massachusetts 02543

ABSTRACT Equilibrium between mitotic microtublues and tubulin is analyzed, using birefringence of mitotic spindle to measure microtubule concentration in vivo. A newly designed temperature-controlled slide and miniature, thermostated hydrostatic pressure chamber permit rapid alteration of temperature and of pressure. Stress birefringence of the windows is minimized, and a system for rapid recording of compensation is incorporated, so that birefringence can be measured to 0.1 nm retardation every few seconds. Both temperature and pressure data yield thermodynamic values ($\Delta H \simeq 35$ kcal/mol, $\Delta S \simeq 120$ entropy units [eu], $\Delta \bar{V} \simeq 400$ ml/mol of subunit polymerized) consistent with the explanation that polymerization of tubulin is entropy driven and mediated by hydrophobic interactions. Kinetic data suggest pseudo-zero-order polymerization and depolymerization following rapid temperature shifts, and a pseudo-first-order depolymerization during anaphase at constant temperature. The equilibrium properties of the in vivo mitotic microtubules are compared with properties of isolated brain tubules.

INTRODUCTION

In contrast to the relatively stable and repeatedly operable force-generating structures found in muscle and flagella, the mitotic spindle is a transient structure. It is newly assembled each time a cell prepares to divide and is disassembled with completion of mitosis. The fibrous elements of the mitotic spindle provide the transient, structural framework and force-producing system which position and distribute chromosomes and other organelles.

The spindle fibers are birefringent and can be visualized with a sensitive polarizing microscope. At each division of a living cell, birefringent fibers can be seen to arise, dynamically organize into the mitotic spindle, and distribute chromosomes and organelles to the daughter cells. These events are vividly displayed in time-lapse motion pictures of developing eggs, spermatocytes, pollen mother cells, and endosperm cells, for example, as in film sequence 1, 3–5 shown at the Minneapolis meetings. (See Inoué,

1964; Inoué and Sato, 1967; Sato and Izutsu, 1974; and Fuseler, 1975, for photographs and description of birefringence changes.)

In electron micrographs, spindle fibers appear as a bundle of ca. 24 nm diameter tubular protein filaments, or microtubules. The oriented array of microtubules accounts for the positive birefringence of spindle fibers[1] (Sato et al., 1971; reviewed by Inoué and Ritter, 1975). In living dividing cells, the change of spindle birefringence reflects fine-structural reorganization of spindle fibers, and in many cases the assembly and disassembly of mitotic microtubules (reviewed in Inoué and Ritter, 1975).

In addition to the organizational changes of spindle fibers which occur naturally during mitosis, one can artificially induce rapid disassembly or assembly of mitotic microtubules. Cold, hydrostatic pressure, colchicine, and Colcemid (Ciba Pharmaceutical Company, Summit, N.J.) can abolish birefringence, depolymerize mitotic microtubules, and halt mitosis in 1–2 min. Removal of these depolymerizing agents, even after prolonged application, allows rapid microtubule reassembly, spindle reorganization, and resumption of mitosis. Protein synthesis is not required for reassembly, and the normal amount of mitotic microtubules can be reversibly doubled or even further increased by temperature elevation or by addition of D_2O (Inoué and Sato, 1967) or glycols (Rebhun et al., 1974). In living cells therefore, mitotic microtubules exist in an equilibrium with a pool of polymerizable subunits (Inoué, 1964; Inoué and Sato, 1967), presumably the 110,000 mol wt heterodimer of tubulin (see e.g., Bryan, 1974).

In 1972 Weisenberg successfully polymerized microtubules in vitro in solutions of tubulin extracted from brain. The microtubules were reversibly disassembled by cold, their polymerization was inhibited by colchicine and the repolymerized microtubules were microscopically undistinguishable from native tubules (reviewed by Olmsted and Borisy, 1973 *a*).

In the present article we report our contribution to the in vivo quantitation of the equilibrium system and discuss its thermodynamic significance. The general features of the in vivo equilibrium system, the justification for using birefringence measurements for study of the equilibrium, and the significance of the equilibrium system to chromosome movements are discussed in a companion article (Inoué and Ritter, 1975).

TEMPERATURE CONTROL AND RETARDATION RECORDING SYSTEM

Time-lapse film sequence 2 shown at the Minneapolis meetings demonstrates the rapid disappearance of spindle birefringence in sea urchin (*Lytechinus variegatus*) eggs exposed to cold, and upon warming, the quick reappearance of birefringence followed by normal cell division (Fig. 1 and 19). Photographic recording and measurement of the low values of spindle birefringence (retardation $< \lambda/1{,}000$) during these transient changes necessitated the development of a new, stress birefringence-free temperature

[1] Sato, H., G. W. Ellis, and S. Inoué. 1975. Microtubular origin of mitotic spindle form birefringence. Submitted for publication.

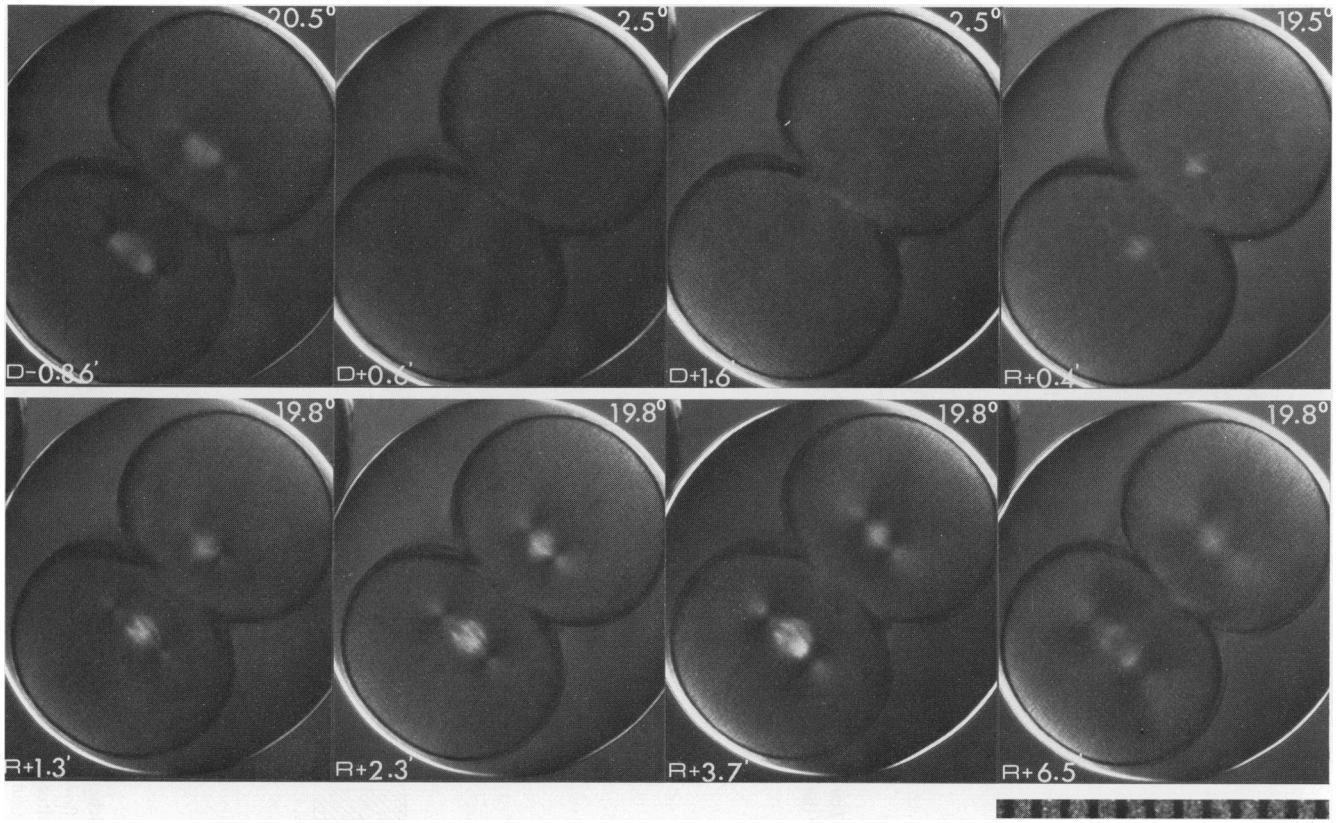

FIGURE 1 Two-cell stage sea urchin *Lytechinus variegatus* eggs exposed to cold during prometaphase (upper cell) and metaphase (lower cell). At time *D*, temperature is dropped from 20.5°C to 2.5°C. Spindle birefringence disappears in ca. 1 min. After 6.2 min in the cold the cell is rewarmed to 19.8°C at *R*. Birefringence recovers rapidly, the spindle is reformed, and anaphase progresses (at $R + 6.5$ min in the lower cell). Time in minutes. Scale interval 10 μm.

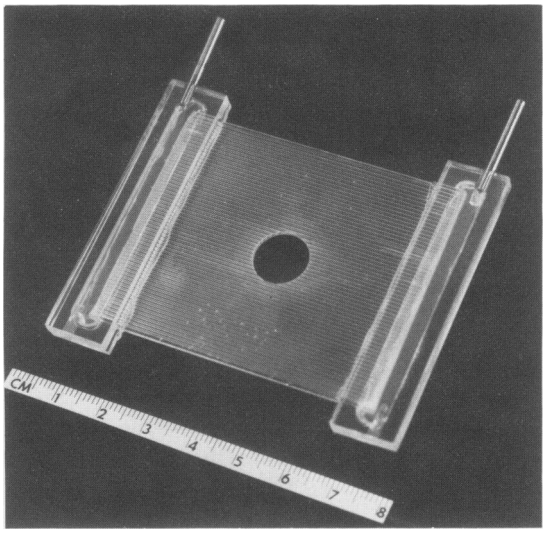

FIGURE 2 Temperature control slide before mounting the two 22 × 22 mm stress-free glass slips which cover the viewing port in the middle of the slide.

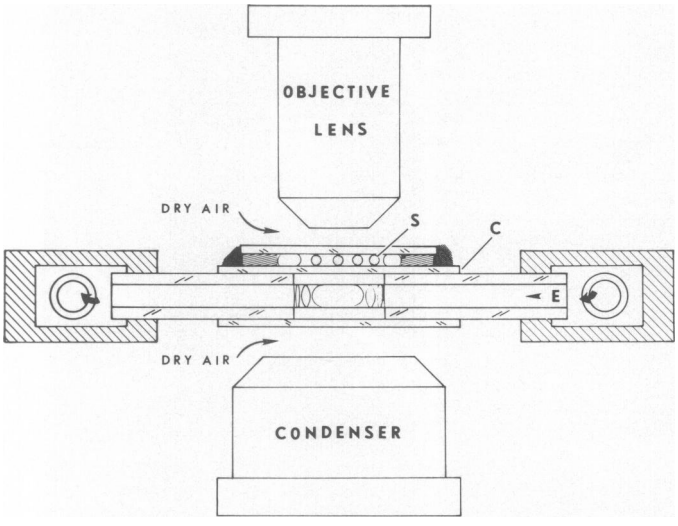

FIGURE 3 Schematic cross section of temperature control slide. Temperature controlled 50% ethanol (*E*) flows through the slide. Specimen (*S*), sandwiched between two cover slips in a column of culture medium surrounded by humidity-equilibrated gas phase, is separated from the alcohol solution by a single 0.17 mm thick cover glass (*C*) and closely follows the alcohol temperature as shown in Fig. 7.

control slide and a system for measuring retardation every few seconds (Inoué, et al., 1970).

A temperature control slide of the following construction permitted rapid shift of temperature upwards and downwards, free from stress birefringence due to differential or anisotropic expansion. A single row of about 40, 0.8 mm OD glass capillaries laid side by side was bonded with silicone or epoxy cement between two, 75 × 35 mm cover slips, previously etched on their inner faces for improved adhesion. The viewing port, a 10 mm diameter hole cut with an abrasive jet through the center of the glass laminate, was covered on both sides with 22 × 22 mm birefringence-free coverslips. The two ends of the laminate where the capillaries open were cemented into two plastic manifolds containing, respectively, the inflow and exit pipes for the temperature control fluid (Fig. 2). The specimen were mounted externally against the 22 × 22 mm glass slip covering the 10 mm port as shown in Fig. 3.

Through this slide, temperature-regulated fluid (50% ethanol) is perfused as shown in Figs. 4 and 5. Fluid from the thermostatically controlled hot and cold reservoirs flows by gravity at a constant rate (100–200 ml/min) to a specially designed mixing

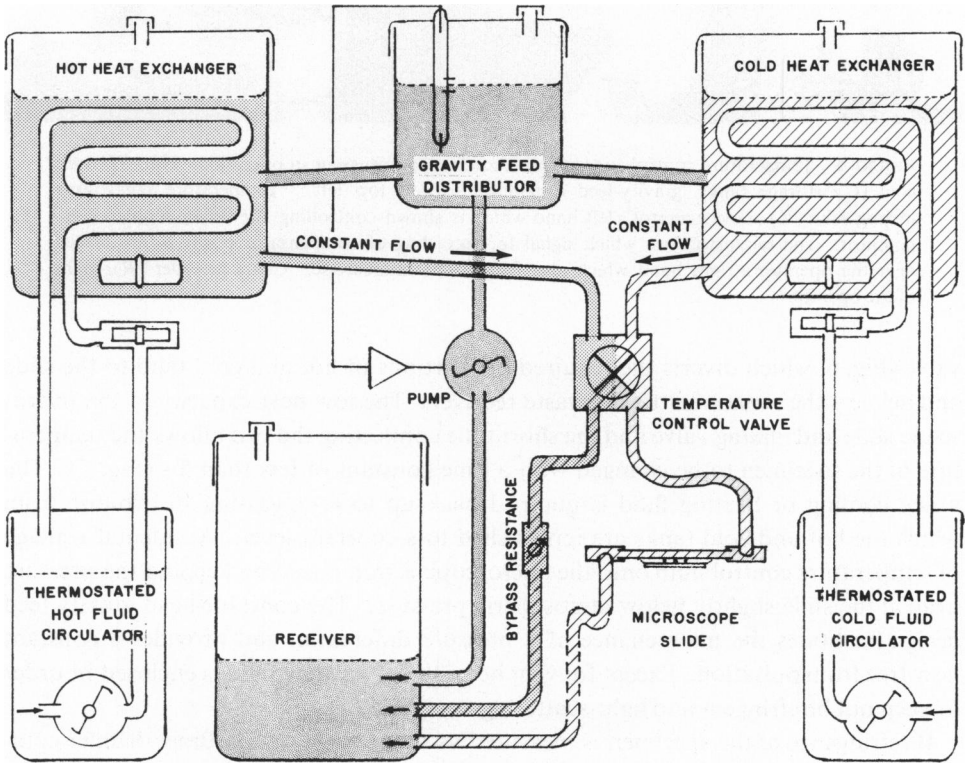

FIGURE 4 Schematic diagram of temperature control system.

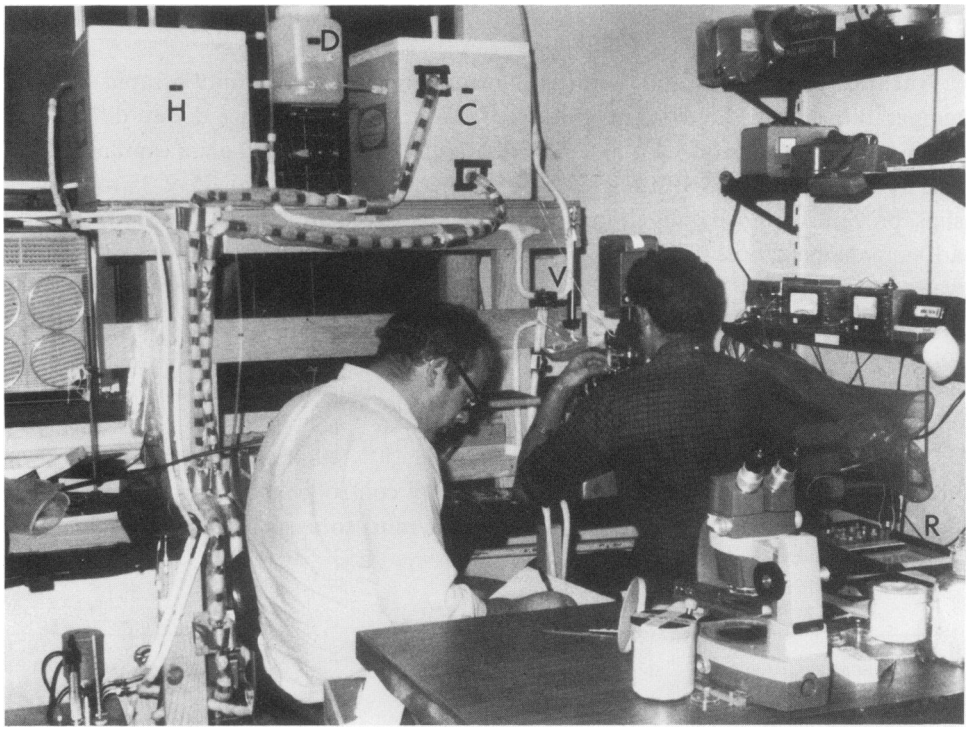

FIGURE 5 Temperature control system and recording compensator in operation. Hot (*H*) and cold (*C*) storage tanks, gravity-feed distributor (*D*) at top left. Temperature controlling mixing valve (*V*) above operator's left hand which is shown controlling the Brace-Köhler compensator. The microswitches, which signal for recording of compensator position, are placed near the operator's right hand which also focuses the microscope. Chart recorder (*R*), right of the operator.

valve (Fig. 6) which diverts the required proportions of hot and cold fluid to the slide and delivers the remainder to the waste receiver. The low heat capacity of the microscope slide and mixing valve and the short tube connecting the two allows the temperature of the specimen to be changed with a time constant of less than 3 s (Fig. 7). The waste cooling or heating fluid is pumped back up to a de-gassing distributor from which the hot and cold tanks are replenished to a constant level. Accidental spillage of temperature control fluid onto the microscope is minimized by keeping the pressure head at the slide slightly below atmospheric pressure. The constant-head gravity feed design facilitates the maintenance of a pressure differential and provides a constant flow free from pulsation. Except for vent holes the circulating fluid is enclosed in order to keep out birefringent and light-scattering contaminants.

Birefringence of the specimen is measured as retardation with a Brace-Köhler compensator (see e.g., Hartshorne and Stuart, 1960) on whose control axis we mounted a miniature precision potentiometer. Supplied with a constant DC voltage, the linear potentiometer provides a voltage output proportional to the compensator orientation.

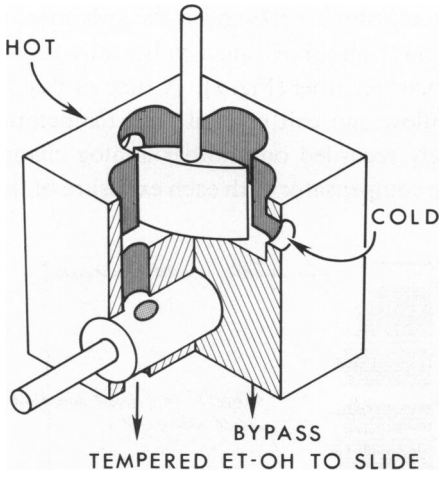

FIGURE 6 Schematic cut-away view of temperature-control mixing valve. Top, front and back covers and O-ring gaskets are not shown. The body of the valve is machined out of polycarbonate resin for alcohol resistance. Temperature of the 50% ethanol (ET-OH) to be perfused is regulated by the top spindle; boat shaped vane proportions hot and cold solutions so that the flow rate through the slide and the bypass circuit each remain constant. The lower valve controls the amount of flow and the pressure head at the slide.

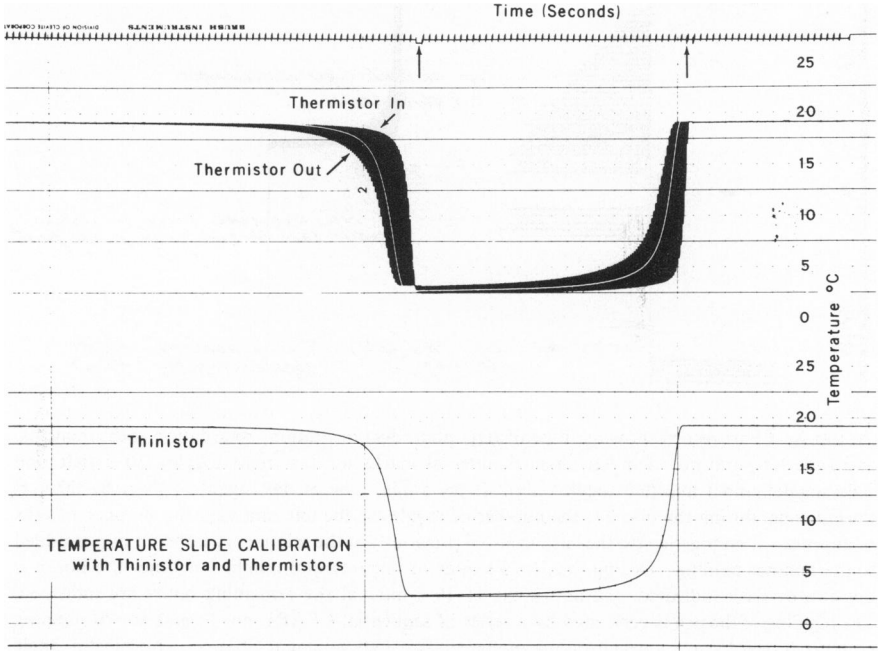

FIGURE 7 Chart record showing response time of temperature control slide. The temperatures of the alcohol solution, measured by thermistor beads placed in the stream near the in-flow out-flow ports of the slide, are alternately monitored four times a second and displayed on the upper analogue channel. The output of a thin, flat thermistor (Thinistor, Victory Engineering Corp., Springfield, N.J.) mounted in place of the specimen is recorded on the lower channel. The time constant for shifting temperature up or down as detected by the Thinistor is about 3 s. At equilibrium the specimen temperature is within 0.1°C of averaged in-flow out-flow solution temperatures.

Once the compensator is adjusted to extinguish the specimen, the observer actuates a microswitch which triggers a one-shot timed pulse thus recording the compensator orientation onto a strip chart recorder (Fig. 8). A time of day signal is recorded by an event marker and the inflow and exit control fluid temperature, measured by small thermistors, are alternately recorded on another analog channel. The recorder also registers the setting of the compensator with each exposure of the still or movie camera.

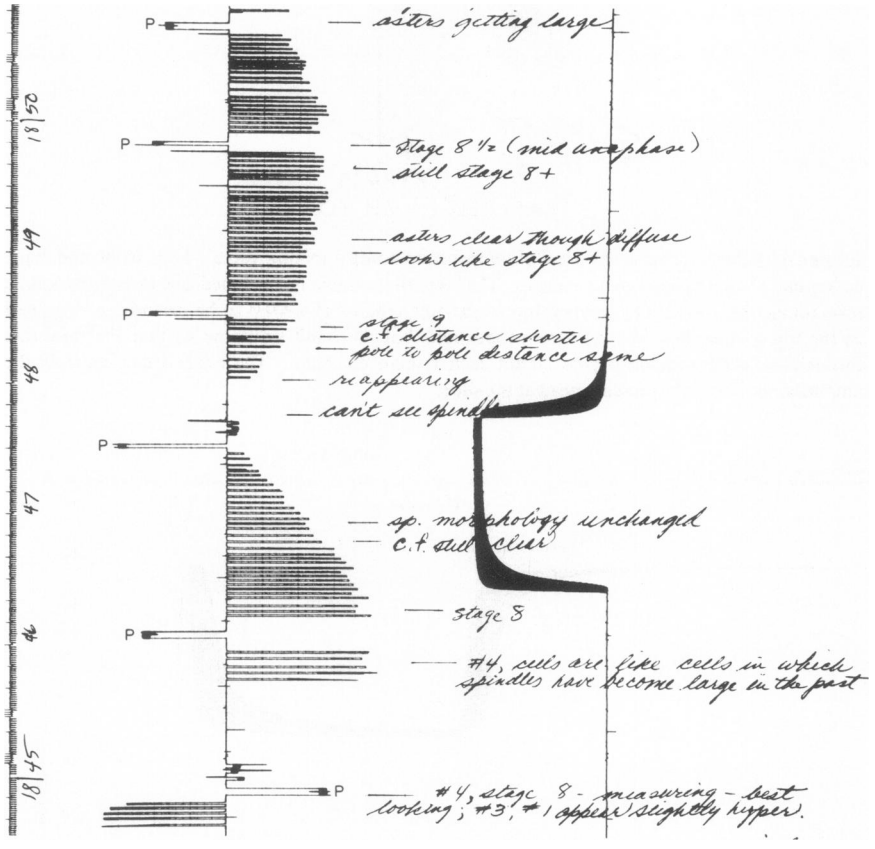

FIGURE 8 Chart record showing: time of day, photodocumentation, retardation measurements, and slide temperature. Far left channel, interval marks for 1 s (right toggle), 10 s (left and right toggle), and 1 min (left toggle only). Every 5 min, time of day signal is given by the following code: during the first 9 s, the number of toggles to the left indicates the number of tens of minutes—if no toggling (to the left) occurred previously at the minute mark then 5 min is added to the minutes reading. During the 21–29 s interval, the intergral number of times the hours is divisible by six is indicated, and during the 11–19 s interval the remaining hours are indicated. The toggling of the pen is generated by a series of sequential CLARE no. 11 and no. 26 stepping switches driven by a 1 s synchronous motor timer. Left analogue channel, compenstor angle measuring spindle extinction (1 s bars), background extinction (short 2 s bars), and compensator setting during photographic exposure (*P*). Although not shown here, photoexposure also toggles far right event marker. Width of bar indicates duration of exposure. Right analogue channel, slide temperature as described for Fig. 7.

THERMODYNAMICS OF THE EQUILIBRIUM SYSTEM

When a cell in mitosis is chilled to an intermediate temperature rather than to a temperature so low as to completely depolymerize the spindle microtubules, the spindle birefringence reaches an intermediate value as shown in Fig. 9. The same equilibrium value is reached whether the final temperature is approached from above or below. Johnson and Borisy (1975) recently showed, for a purified solution of tubulin extracted from brain, that microtubules in vitro can also be in a true equilibrium with the 110,000 mol wt (hetero-) dimer of tubulin.

As shown earlier (Inoué, 1959), the equilibrium birefringence of a metaphase arrested spindle in the oocyte of *Chaetopterus* approaches a plateau value (A_o) at the higher range of physiological temperatures. These data, relating equilibrium retardation to temperature, are plotted in Fig. 10 together with recent data on *Chaetopterus* obtained by Salmon (1975). The solid, sigmoid curve shown in Fig. 10 was theoretically specified by the straight line in Fig. 11 as discussed below.

The birefringence (B) measures the concentration of tubulin in the oriented microtubules (Inoué and Ritter, 1975; Sato et al., 1971, 1975). Concentration of the free subunits is given by ($A_o - B$) since A_o represents the tubulin concentration when the equilibrium is pushed all the way towards the polymer.

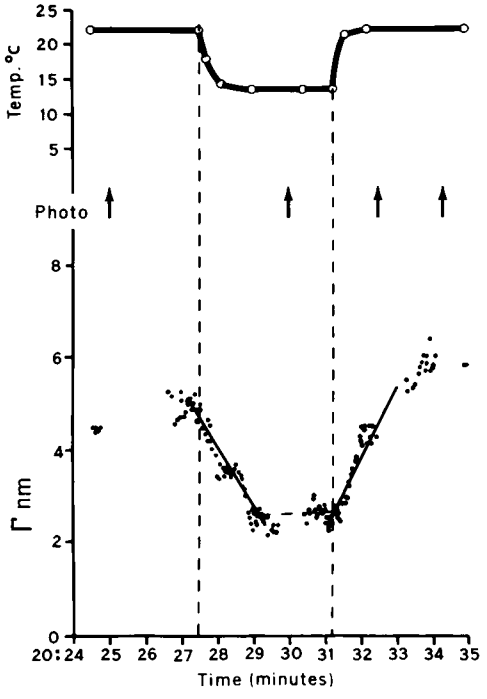

FIGURE 9 Birefringence measured as retardation (Γ) of a metaphase-blocked spindle in a *Chaetopterus* oocyte treated with 45% D_2O sea water and then chilled from 22.5° to 13.5°C. Equilibrium retardation is reached within 2 min.

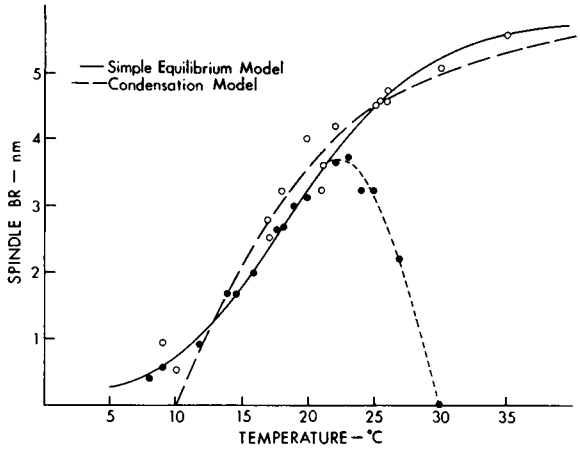

FIGURE 10 Equilibrium values of *Chaetopterus* oocyte spindle retardation vs. temperature. Open circles from Inoué, (1959), solid circles from Salmon (1973). The solid curve is defined by Eq. 4 and plotted for constant ΔH and ΔS values obtained by least squares fitting of data as shown in Fig. 11. For a discussion on the fit of the broken curve "condensation model" see Salmon (1975). (From Salmon, 1975.)

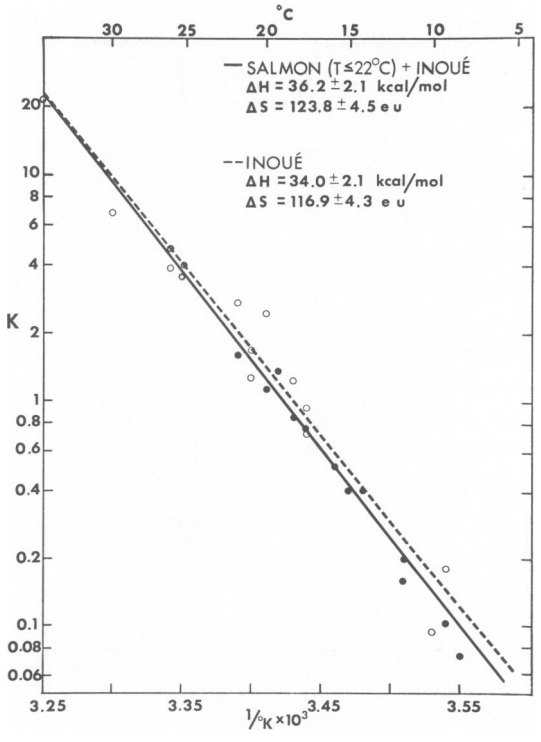

FIGURE 11 Data in Fig. 10 shown as van't Hoff plot: $K = \ln [B/A_o - B)]$ vs. inverse absolute temperature. A_o is high temperature asymtote in Fig. 10. (From Salmon, 1975.)

Thus

$$A_o - B \overset{K(T,P)}{\rightleftharpoons} B. \tag{1}$$

The equilibrium constant $K(T,P)$ is given by

$$K(T,P) = [B]/[A_o - B]. \tag{2}$$

Since the free energy change (ΔG^o) of an equilibrium chemical system is given by:

$$K(T,P) = e^{-\Delta G^o/RT},$$
$$-\Delta G^o = RT \ln K(T,P) = RT \ln ([B]/[A_o - B]). \tag{3}$$

At 1 atm, the Gibbs free energy ΔG_1^o is:

$$\Delta G_1^o = \Delta H - T\Delta S,$$

where ΔH is the enthalpy increment, T is the absolute temperature, and ΔS is the entropy change per mole of reactant. Combined with Eq. 3,

$$-\ln ([B]/[A_o - B]) = (\Delta H/RT) - (\Delta S/R). \tag{4}$$

As shown in Fig. 11, the van't Hoff plot, or $\ln [B/(A_o - B)]$ plotted against $1/T$, yields a straight line whose slope provides a ΔH value of 35 kcal/mol of subunit associated, and its intercept gives a positive ΔS of 120 entropy units (eu).

These measurements were made on metaphase arrested spindles in *Chaetopterus* oocytes. Similar thermodynamic behavior has been observed in active metaphase spindles of plant and animal cells, both in meiosis and in mitosis (Stephens, 1973; Fuseler, 1973 *a*). In all cases, polymerization is accompanied by a high positive entropy (ΔS = 100–300 eu) and positive enthalpy (ΔH = 25–40 kcal). At physiological temperatures the free energy (ΔG^o) released upon polymerization is less than 1 kcal/mol.

This endothermic, entropy driven reaction appears to reflect destructuring of water from the tubulin subunits upon polymerization. In other words the assembly of microtubules appears to be driven by hydrophobic interactions. Similarly high values of positive ΔH and ΔS are characteristically observed in hydrophobic associations of proteins generally.

As with several other hydrophobically mediated protein polymerizing systems, equilibrium between tubulin and microtubules is shifted towards polymerization by heavy water, with peak effect at ca. 45% D_2O volume concentration (Inoué and Sato, 1967; Olmsted and Borisy, 1973 *b*). Compared with H_2O, D_2O forms a tighter association with itself (e.g., Sidgwick, 1950) and forms micelles at lower concentration of detergent than in H_2O (Kresheck et al., 1965).

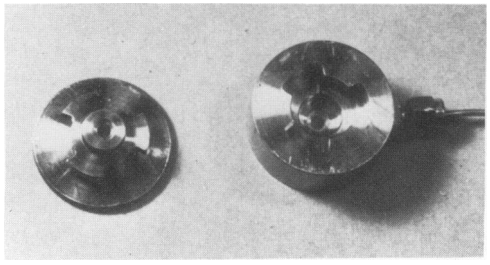

FIGURE 12

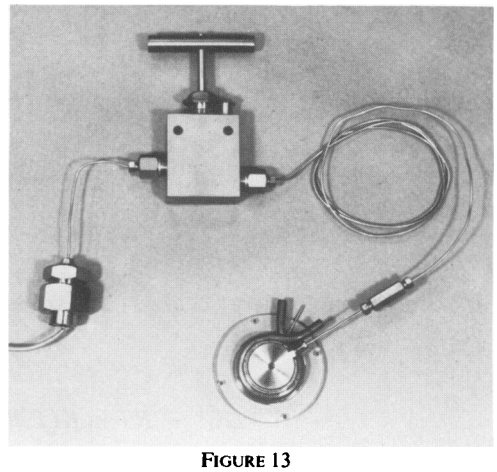

FIGURE 13

FIGURE 12 Miniature pressure chamber designed for use with polarization and phase contrast microscopes shown inverted with bottom (left) removed. At 5,500 lb/in^2, window stress birefringence is still sufficiently low to permit polarized light observations of spindle birefringence in living cells. Total retardation of the spindle at 1 atm is less than one hundredth of a wave length of light. (From Salmon and Ellis, 1975.)

FIGURE 13 Microscope pressure chamber with "pump" and pressure gauge attached. Because of the very small displacement volumes involved, several thousand pounds per square inch of pressure can be generated by a single turn of a needle valve (center of photo) which replaces a conventional pump. The double hexagonal unit to the left, houses the strain-gauge pressure transducer whose electrical resistance provides the pressure reading. (From Salmon and Ellis, 1975.)

PRESSURE INDUCED CHANGE OF EQUILIBRIUM

Thermodynamic analysis of the polymerization equilibrium in *Chaetopterus* spindle was extended, using pressure as a variable. A new microscope chamber (Figs. 12–14) permits rapid application of hydrostatic pressures up to 15,000 lb/in^2, with sufficiently low window stress birefringence to permit polarized light microscopy of spindles up to ca. 5,500 lb/in^2 and phase contrast observation of chromosomes up to ca. 10,000 lb/in^2 (Salmon and Ellis, 1975).

In living cells, application of hydrostatic pressure reduces spindle fiber birefringence signaling the depolymerization of spindle microtubules. As with temperature, birefringence change is totally reversible and a *Chaetopterus* egg subsequently fertilized can develop as a normal embryo.

At constant temperature, an equilibrium birefringence is reached for each given pressure (Fig. 15). The equilibrium retardation measured at three temperatures is shown in Fig. 16. As the figure shows, the data closely fit theoretical curves derived from Eqs. 2 and 5 for a constant molar volume increment of association ($\Delta \bar{V}$) of 400 ml/mol of polymerizing subunit. $\Delta \bar{V}$ was derived from the van't Hoff plots as described below.

When pressure is altered, the thermodynamic Eq. 3 takes the general form (Salmon, 1975),

$$-\ln K(T,P) = \Delta G_1^\circ/RT - (P - 14.7)\,\Delta \bar{V}/RT, \qquad (5)$$

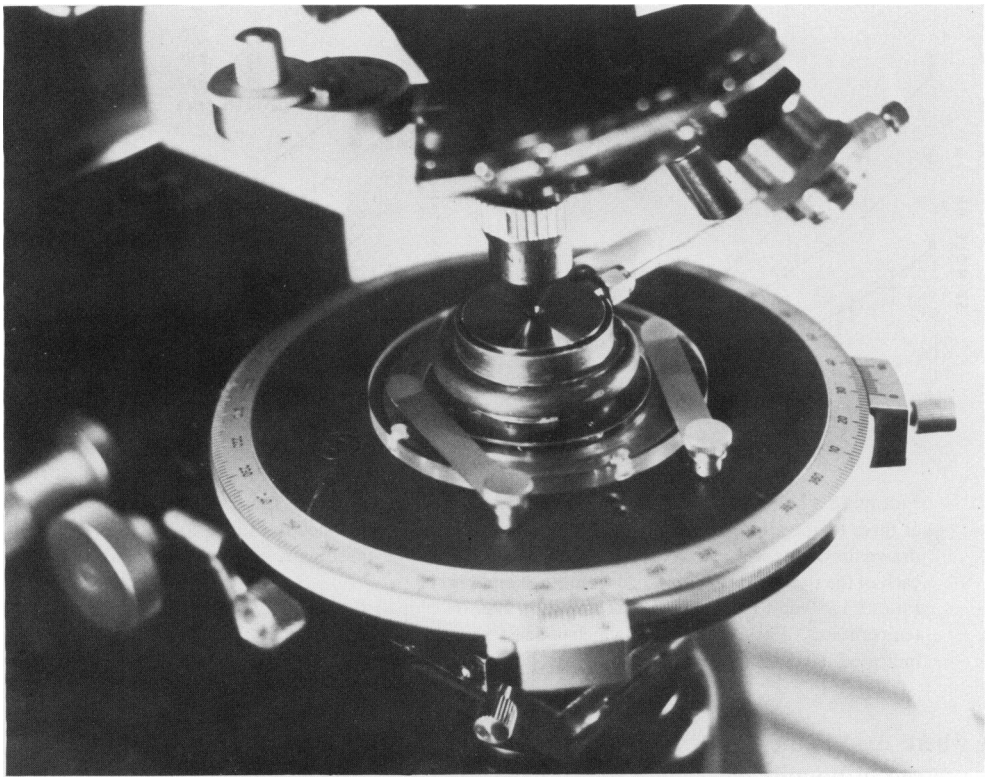

FIGURE 14 Pressure chamber mounted on the stage of a polarizing microscope. The chamber fits in a water jacketed sleeve. (From Salmon and Ellis, 1975.)

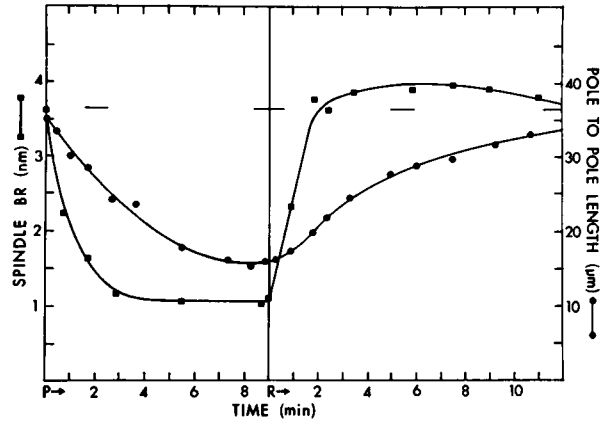

FIGURE 15 Birefringence retardation and length of *Chaetopterus* spindle exposed at *P* to 2,000 lb/in^2. At *R* pressure is returned to 1 atm (=14.7 lb/in^2). (After Salmon, 1975.)

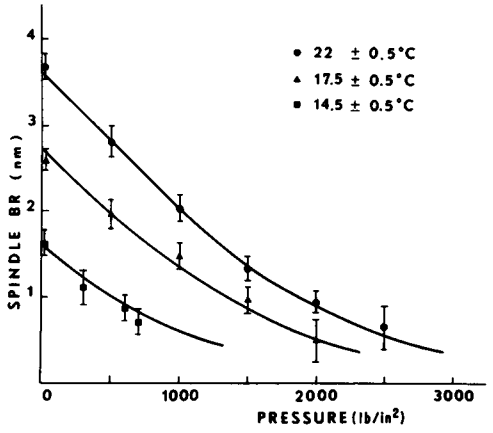

FIGURE 16

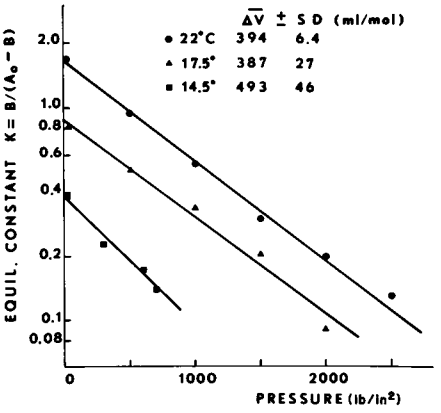

FIGURE 17

FIGURE 16 Equilibrium retardation measured as function of pressure for *Chaetopterus* spindle at three temperatures. The three curves are theoretical curves defined by Eqs. 2 and 5, and are drawn for constant molar volume increments of 400 ml/mol of subunit polymerized. ΔG_1° for each of the three curves is obtained from Eq. 3 and Fig. 11.

FIGURE 17 van't Hoff plot of data shown in Fig. 16; plotted as ln $[B/(A_o - B)]$ vs. P for three temperatures. Each straight line which is least squares fitted to the data, yields the $\Delta \bar{V}$ value indicated. (After Salmon, 1975.)

where ΔG_1° is the Gibbs free energy at 1 atm (=14.7 lb/in^2, and pressure P is expressed in pounds per square inch. Consistent with this equation for constant ΔV and with ln $K(T,P)$ as defined by Eq. 2 ln $[B/(A_o - B)]$ plots against P as a straight line for each temperature (Fig. 17). Measurements made at three temperatures yield straight lines displaced as predicted from Eqs. 2 and 5 and the values of ΔG_1° obtained by varying temperature at unit atmosphere.

The molar volume change ($\Delta \bar{V}$) is given by the slope of the lines as ca. 400 ml/mol (Fig. 17). This value, as with the ΔH and ΔS values, is comparable with the molar volume changes of association seen in other hydrophobic, entropy-driven polymerization systems such as tobacco mosaic virus, flagellin, and actin. Depending on the system involved, however, different equations have been used to describe the polymerization-depolymerization equilibria (see Stephens, 1973; Fuseler, 1973*a*; Salmon, 1975; and Johnson and Borisy, 1975, for discussions of this point and for tables comparing thermodynamic parameters for the various entropy-driven, polymerization systems).

KINETICS OF SPINDLE RETARDATION CHANGE

Figs. 18 and 19 illustrate the kinetic changes of spindle retardation upon sudden chilling, sudden rewarming, and as seen in natural anaphase at constant temperature. In this sea star (*Asterias forbesi*) egg cooled at −1°C, the retardation of the spindle fibers, measured halfway between the pole and chromosomes, decays lineraly to zero at approximately 3.3 nm/min; upon rewarming to 17°C, retardation recovers at the same

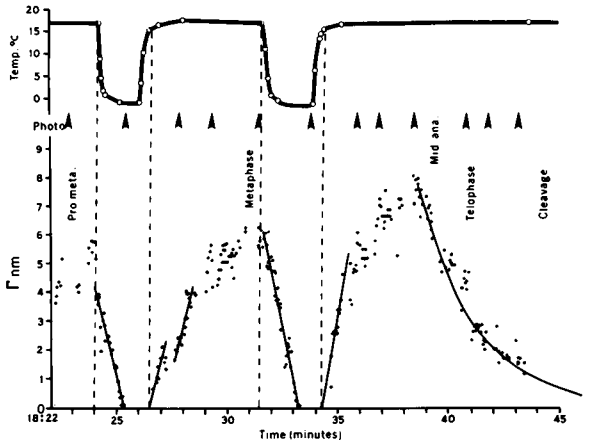

FIGURE 18 Birefringence changes, measured as retardation (Γ), of mitotic spindle in the egg of a sea star *Asterias forbesi*. The first two drops in retardation measure the rapid depolymerization of mitotic microtubules upon chilling. Upon rewarming, spindle birefringence recovers just as fast as it disappeared, reflecting the rapid reassembly of microtubules. After initial reassembly, retardation fluctuates as spindle is reorganized (see Fig. 1). The third drop in retardation takes place without chilling. This reflects the natural depolymerization of microtubules in anaphase. The anaphase retardation decay is logarithmic in contrast to the linear decay induced by sudden chilling.

rate linearly, until fiber reorganization gives rise to secondary changes. Similar "pseudo-zero-order" kinetics have been observed on spindle isolated in tubulin-containing solutions and depolymerized in vitro by sudden chilling (Inoué et al., 1974).

Taken at face value this pseudo-zero-order decay would seem to suggest: (*a*) that the monomer-polymer equilibrium between tubulin and microtubules is shifted strongly in favor of the monomer so that little impetus toward repolymerization is felt by the depolymerizing tubules; and (*b*) that depolymerization is confined to tubule ends (so that depolymerization proceeds from a fixed number of sites) rather than elsewhere along the tubule. We view this interpretation with some reservation, however, since Gaskin et al. (1974) have shown that the number of microtubule ends increased by sonic fragmentation does not alter the rate of cold induced depolymerization in vitro. Johnson and Borisy (1975) on the other hand find enhanced depolymerization by cold in more mildly sheared microtubule solutions. In vivo, the retardation appears to drop uniformly along the length of fibers when cells are chilled sufficiently rapidly so that the fibers do not shorten during chilling (see Fig. 1 and Inoué and Ritter, 1975).

The rates of retardation change vary within a limited range in cells from different species but are relatively unaffected by the medium in which the cell is immersed (Table I). Mitotic stage-dependent variation is consistently observed for some cells but a fixed pattern has not yet emerged for different cell types.

In contrast to the linear retardation decay encountered in cold-induced depolymerization, the spontaneous retardation decay seen in anaphase follows a logarithmic course (Fig. 18). The retardation decay in colchicine (and Ca^{++}) induced depolymeri-

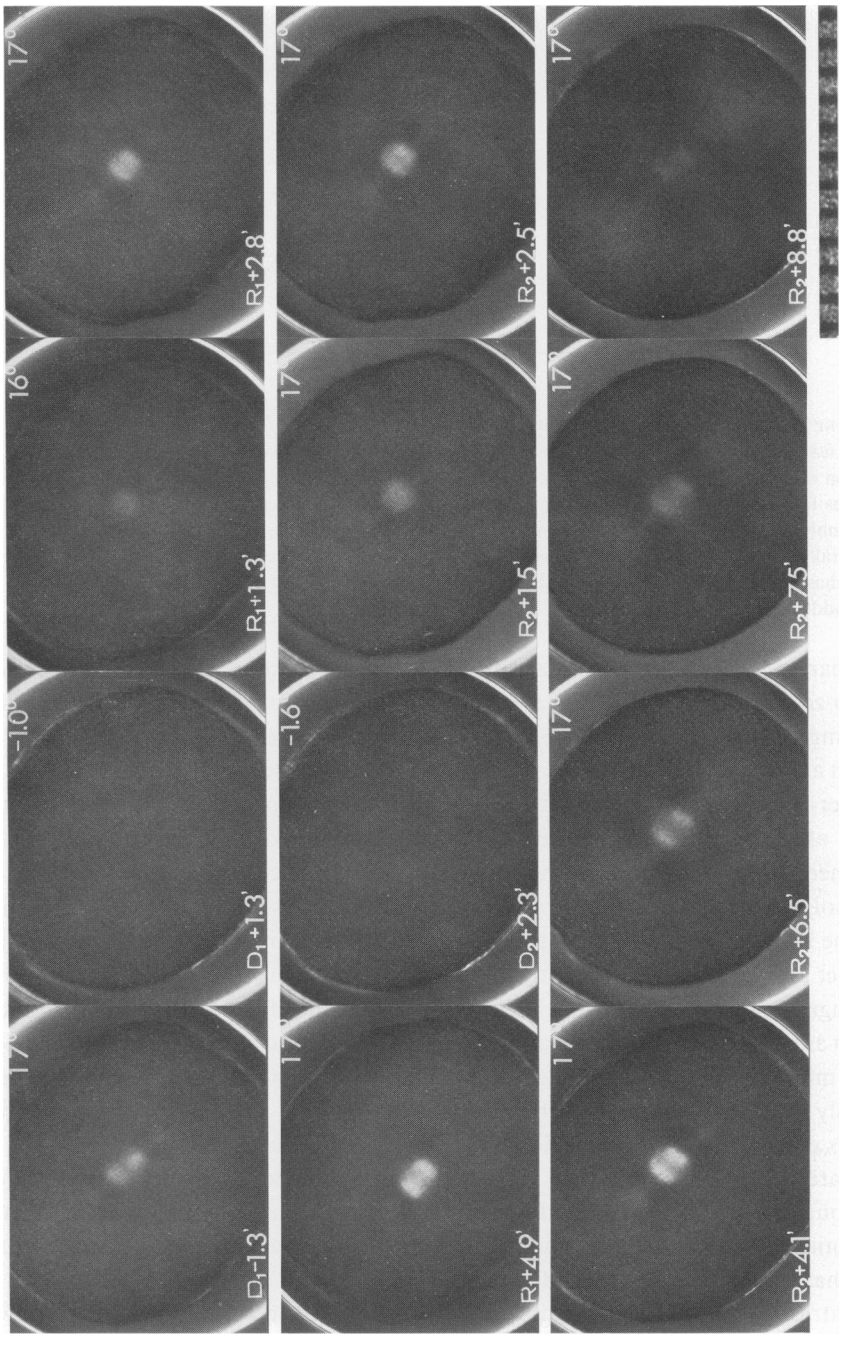

FIGURE 19 Photographs of *Asterias* egg taken at the times indicated by arrows in Fig. 18.

TABLE I

RATE OF RETARDATION CHANGE OF MITOTIC SPINDLE IN VIVO UPON SUDDEN DROP OR RISE OF TEMPERATURE

Cells	Temperature		Retardation change rate for step change in temperature		No. of cells	Observed in
	Upper	Lower	Drop	Rise		
PLANT ENDOSPERM	°C		nm/min			
Haemanthus katherinae						
Meta.	20	4	1.4 ± 0.3	1.3 ± 0.4	6	Endosperm fluid
Phragmopl.	20	4	0.5 ± 0.1	0.4 ± 0.1	3	Endosperm fluid
Tilia americana						
Meta.	22	3.5	1.9 ± 0.5	2.2 ± 0.8	5	Endosperm fluid
Phragmopl.	22	2	1.4 ± 0.6	2.4 ± 1.1	2	Endosperm fluid
ANIMAL CELLS						
Meiotic metaphase oocytes						
Asterias forbesi	18	0.5	2.5 ± 0.9	1.8 ± 0.6	8	A.S.W.
	18	0.5	2.4 ± 0.8	1.6 ± 0.5	10	45% D_2O-A.S.W.
	18	0.5	2.5 ± 0.5	1.4 ± 0.4	9	Low Ca, D_2O-S.W.
Meiotic meta. arrested oocytes						
Pectinaria gouldi	24	0.5	3.3 ± 0.8	2.3 ± 0.3	8	A.S.W.
Chaetopterus pergamentaceous	24	0.4	5.1 ± 0.8	2.5 ± 0.8	4	A.S.W.
Spermatocytes, meiosis I						
Nephrotoma sp. Meta.	20	11	0.4 ± 0.2	0.4 ± 0.1	4	Testis fluid in Kel-F10 oil
" Meta.	20	1.8	0.8 ± 0.2	1.9 ± 0.5	9	Testis fluid in Kel-F10 oil
" Ana.	20	1.8	1.0 ± 0.1	1.1 ± 0.1	5	Testis fluid in Kel-F10 oil
Cleavage mitosis metaphase						
Lytechinus variegatus	20	1	4.9 ± 1.4	4.2 ± 0.8	9	A.S.W.
	17.5	1.7	4.9 ± 0.9	3.8 ± 0.8	13	30% D_2O-A.S.W.
	20	2.2	6.0 ± 1.7	3.5 ± 1.0	10	Ca-free-A.S.W.
	17.7	1	4.7 ± 0.1	3.0 ± 0.5	4	1 mM Caffeine-A.S.W.
Asterias forbesi	18	1	4.3 ± 1.6	2.5 ± 1.2	17	A.S.W.
	18	1	3.6 ± 1.5	2.6 ± 0.9	5	45% D_2O-A.S.W.
	18	1	3.3 ± 1.2	2.7 ± 1.1	6	55% Ca-A.S.W.
	18	1	3.3 ± 1.0	1.7 ± 0.4	7	Low Ca, D_2O-S.W.

Meta., metaphase; Ana., anaphase; Phragmopl., phragmoplast; A.S.W., artificial sea water according to Kavanaugh (1956), "Formulae and Methods," Marine Biological Laboratories, Woods Hole, Mass.; Low Ca, D_2O-S.W., 55 vol of A.S.W. mixed with 45 vol of Ca-free D_2O sea water; D_2O, deuterium oxide 99.84% from BioRad Lab, Richmond, Calif.; Kel-F 10, fluorocarbon oil supplied by Minnesota Mining and Manufacturing Co., but now discontinued. Halocarbon HC 10-25, from Halocarbon Products Corp., Hackensack, N.J., has appeared to be an adequate substitute.

zation likewise follows a logarithmic time course in vivo (see Inoué, 1952, for colchicine-induced decay) as well as in vitro (Inoué et al., 1974; Borisy et al., 1974; Haga et al., 1974; Gaskin et al., 1975).

In these cases the reaction is proceeding as though: either (*1*) significant back pressure from subunits rate limits depolymerization, or (*2*) the equilibrium is otherwise limited by a first-order reaction. D_2O and temperature step-up experiments which we have performed favor the second interpretation for anaphase birefringence decay.

The time constant for the logarithmic retardation decay in anaphase is a sensitive, nonlinear function of temperature. The same function governs the velocity of anaphase chromosome movement. This observation plays an important role in considerations of chromosome movement mechanisms (Fuseler, 1973 *a* and *b*; Inoué and Ritter, 1975).

DISCUSSION

We are today not yet in a position to compare directly the kinetics of the in vitro assembly system with mitotic microtubule assembly in vivo. The in vivo system is in a dynamic rather than static equilibrium (Inoué and Ritter, 1975). In the in vitro system nucleation steps affect the kinetics of polymerization. In vivo, the need for spontaneous nucleation may be circumvented by the presence of specialized nucleating sites such as centrioles and kinetochores or by other cellular control mechanisms (see Inoué, 1964; Inoué and Sato, 1967; Pickett-Heaps, 1969; and Weisenberg, 1973, 1975).

These reservations notwithstanding, equilibrium behavior of the in vitro tubulin-microtubule assembly system is found to parallel the in vivo system to a remarkable degree (reviewed in Olmsted and Borisy, 1973 *a*; Inoué and Ritter, 1975; and Johnson and Borisy, 1975).

The dynamic equilibrium concept offers valuable insight into the properties of the mitotic spindle and related labile microtubular systems in living cells. We have shown that it describes the behavior of the spindle in response to changes in temperature and pressure, and a variety of chemical agents that affect the equilibrium. To lengthen, microtubules must polymerize more tubulin; to shorten, the tubulin polymer must be depolymerized. Since the mechanical connection of chromosomes to the spindle has been shown to be coextensive in time and space with the birefringent (microtubular) chromosomal fiber (Begg and Ellis, 1974), chromosome movement involving chromosomal fiber shortening without thickening must at least be rate limited by microtubule depolymerization. We have long suggested that microtubule depolymerization may provide the motive force for this type of chromosome movement.[2] We now have found that by regarding the microtubule as a cylindrical micelle, we can, through the

[2] At the Biophysics-Biochemistry Society Meeting, time-lapse motion pictures demonstrating the following were shown in addition to sequences 1–5 already described in the text. Sequence 6: 3 mM colchicine induces depolymerization and shortening of *Chaetopterus pergamentaceous* spindle fibers, resulting in transport of chromosomes to the cell cortex to which the outer spindle pole is anchored by its astral rays. 5 mM Colcemid dissolves the spindle *in situ* without appreciable fiber shortening or chromosome transport. Spindle fibers shown with polarized light, chromosomes with phase contrast microscopy. Sequence 7: Colchicine-

use of parameters derived from thermodynamic experiments, provide a model for chromosomal movement in which the interfacial tension developed during the depolymerization of a single microtubule would be sufficient to overcome the viscous drag which is the primary nonmicrotubular impediment to chromosome movement (Inoué and Ritter, 1975).

This paper is dedicated to Aharon Katchalsky and to Wayne Thornburg, two brilliant individuals whose stimulating discussions and friendships shall be dearly missed.

This work was supported in part by National Institutes of Health grant CA-10171 and National Science Foundation grant GB-31739.

REFERENCES

ARONSON, J. F. 1973. Nuclear membrane fusion in fertilized *Lytechinus variegatus* eggs. *J. Cell Biol.* **58**:126.

BEGG, D. A., and G. W. ELLIS. 1974. The role of birefringent chromosomal fibers in the mechanical attachment of chromosomes to the spindle. *J. Cell Biol.* **63**:18*a*.

BORISY, G. G., J. B. OLMSTED, J. M. MARCUM, and C. ALLEN. 1974. Microtubule assembly *in vitro*. *Fed. Proc.* **33**:167

BRYAN, J. 1974. Biochemical properties of microtubules. *Fed. Proc.* **33**:152.

FUSELER, J. 1973 *a*. The Effect of Temperature on Chromosome Movement and the Assembly-Disassembly Process of Birefringent Spindle Fibers in Actively Dividing Plant and Animal Cells. Ph.D. Thesis, University of Pennsylvania. University of Michigan Film Library, Ann Arbor, Mich.

FUSELER, J. 1973 *b*. Temperature dependence of anaphase chromosome velocity and microtubule depolymerization rate. *J. Cell Biol.* **59**:106*a*.

FUSELER, J. W. 1975. Mitosis in *Tilia americana* endosperm. *J. Cell Biol.* **64**:159.

GASKIN, F., C. R. CANTOR, and M. L. SHELANSKI. 1974. Turbidimetric studies of the *in vitro* assembly and disassembly of porcine neurotubules. *J. Mol. Biol.* **89**:737.

GASKIN, F., C. R. CANTOR, and M. L. SHELANSKI. 1975. Biochemical studies on the *in vitro* assembly and disassembly of microtubules. *Ann. N.Y. Acad. Sci.* In press.

HAGA, T., T. ABE, and M. KUROKAWA. 1974. Polymerization and depolymerization of microtubules *in vitro* as studied by flow birefringence. *FEBS Lett.* **39**:291.

HARTSHORNE, N. H., and A. STUART. 1960. Crystals and the Polarizing Microscope. Edward Arnold Ltd., London.

INOUÉ, S. 1952. The effect of colchicine on the microscopic and submicroscopic structure of the mitotic spindle. *Exp. Cell Res. Suppl.* **2**:305.

INOUÉ, S. 1959. Motility of cilia and the mechanism of mitosis. *Rev. Mod. Phys.* **31**:402.

INOUÉ, S. 1964. Organization and function of the mitotic spindle. *In* Primitive Motile Systems in Cell Biology. R. D. Allen and N. Kamiya, editors. Academic Press Inc., New York. 549–598.

INOUÉ, S., G. G. BORISY, and D. P. KIEHART. 1974. Growth and lability of *Chaetopterus* oocyte mitotic spindles isolated in the presence of porcine brain tubuline. *J. Cell Biol.* **62**:175.

INOUÉ, S., G. W. ELLIS, E. D. SALMON, and J. W. FUSELER. 1970. Rapid measurement of spindle birefringence during controlled temperature shifts. *J. Cell Biol.* **47**:95*a*.

INOUÉ, S., and H. RITTER. 1975. Dynamics of mitotic spindle organization and function. *In* Molecules and Cell Movement. S. Inoué and R. E. Stephens, editors. Raven Press, N.Y. In press.

INOUÉ, S., and H. SATO. 1967. Cell motility by labile association of molecules. *J. Gen. Physiol.* **50**:259.

JOHNSON, K. A., and G. G. BORISY. 1975. The equilibrium assembly of microtubules *in vitro*. *In* Molecules and Cell Movement. S. Inoué and R. E. Stephens, editors. Raven Press, N.Y. In press.

inhibited migration of sea urchin (*Lytechinus variegatus*) pronuclei, was reinitiated by photoconversion of colchicine to the inactive lumicolchicine. The female pronucleus, towards which the male pronucleus migrates in the absence of this treatment, rapidly approached the male pronucleus and syngamy is completed. Differential interference contrast microscopy. (Courtesy Dr. John F. Aronson. See Aronson, 1973).

KRESHECK, G. C., H. SCHNEIDER, and H. A. SHERAGA. 1965. The effect of D_2O on the thermal stability of proteins. Thermodynamic parameters for the transfer of model compounds from H_2O to D_2O. *J. Phys. Chem.* **69**:3132.

OLMSTED, J. B., and G. G. BORISY. 1973 *a*. Microtubules. *Ann. Rev. Biochem.* **42**:507.

OLMSTED, J. B., and G. G. BORISY. 1973 *b*. Characterization of microtubule assembly in porcine brain extracts by viscometry. *Biochemistry.* **12**:4282.

PICKETT-HEAPS, J. D. 1969. The evolution of the mitotic apparatus: an attempt at comparative ultrastructural cytology in dividing plant cells. *Cytobios.* **3**:257.

REBHUN, L. I., M. MELLON, D. JEMIOLO, J. NATH, and N. IVY. 1974. Regulation of size and birefringence of the *in vivo* mitotic apparatus. *J. Supramol. Struct.* **2**:466.

SALMON, E. D. 1973. The Effects of Hydrostatic Pressure on the Structure and Function of the Mitotic Spindle: an in vivo Analysis with a Newly Developed Microscope Pressure Chamber. Ph.D. Thesis, University of Pennsylvania. University of Michigan Film Library, Ann Arbor, Mich.

SALMON, E. D. 1975. Pressure-induced depolymerization of spindle microtubules. II. Thermodynamics of in vivo spindle assembly. *J. Cell Biol.* In press.

SALMON, E. D., and G. W. ELLIS. 1975. A new miniature hydrostatic pressure chamber for microscopy: strain-free optical glass windows facilitate phase contrast and polarized light microscopy of living cells. Optional fixture permits simultaneous control of pressure and temperature. *J. Cell Biol.* **65**:587.

SATO, H., S. INOUÉ, and G. W. ELLIS. 1971. The microtubular origin of spindle birefringence: experimental verification of Wiener's equation. *Proc. 11th Annu. Meeting Am. Soc. Cell Biol.* 261*a* (Abstr.).

SATO, H., and K. IZUTSU. 1974. Birefringence in Mitosis of the Spermatocyte of Grasshopper *Chrysochraon japonicus.* Time-lapse motion picture. Available from George W. Colburn Laboratory, Inc., Chicago, Ill.

SIDGWICK, N. V. 1950. Chemical Elements and Their Compounds. Vol. 1. Clarendon Press, Oxford.

STEPHENS, R. E. 1973. A thermodynamic analysis of mitotic spindle equilibrium at active metaphase. *J. Cell Biol.* **57**:133.

WEISENBERG, R. C. 1972. Microtubule formation *in vitro* in solutions containing low calcium concentrations. *Science (Wash. D.C.).* **177**:1104.

WEISENBERG, R. C. 1973. Regulation of tubulin organization during meiosis. *Am. Zool.* **13**:981

WEISENBERG, R. C., and A. C. ROSENFELD. 1975. In vitro polymerization of microtubules into asters and spindles in homogenates of surf clam eggs. *J. Cell Biol.* **64**:146.